Evaluation of the Turbulence Models for the Simulation of the Flow Over a Tsentralniy Aerogidrodinamicheskey institut (TsAGI)-12% Airfoil

Nishant Kumar[1], Saurav Upadhaya[2], Ashish Rohilla[3]
Department Of Mechanical Engineering, Greater Noida Institute Of Technology, Greater Noida, Uttar Pradesh

Abstract

The numerical analysis of the two-dimensional subsonic flow over a Tsentralniy Aerogidrodinamicheskey institut "B" series (TsAGI) -12% airfoil at an assorted angle of attack (AOA) and flow operating at a Reynolds number of 1×10^6 is proposed. The flow is established by employing the steady-state governing equation of continuity and momentum conservation conflated with one of the four turbulence models [Spalart-Allmaras (1 equation),Standard k-ε (2 equation), k-ω standard (2 equation) and Transition SST (4 equation)]. The intention of the study is to demonstrate the behaviour of the Airfoil at different turbulence models as mentioned furthermore, in addition, to obtain a verified solution method. The computational domain is composed of 43584 structured cells. In order, to properly capture the boundary layer, refinement of the grid near the Airfoil is done. The calculations were made by fixing the velocity (14.6122449 m/s) of the flow at a fixed Reynolds number Re= 1×10^6 and altering the only angle of attack (AOA). The presented work demonstrated the coefficient of lift and coefficient of drag at different turbulence models, at varying angle of attack. In addition, the work also emphasizes that at higher AOA, the turbulence models used in commercial CFD, yet not able to produce accurate results.

Keywords — *Computational Fluid Dynamics (CFD), Coefficient of Drag (C_d),Turbulence models, Boundary layer, Numerical Analysis, Subsonic, Airfoil.*

I. INTRODUCTION

An extensive amount of research has been made on computational fluid dynamics (CFD) from past few decades, also due to the rapid growth in the calculating ability of the available calculating resources has made this possible. The necessity of faster and much accurate method of calculating the flow fields around configuration of technical interest has made computational fluid dynamics (CFD) a comfortable choice for designers in the field of Aerospace, Automotive and industrial components industry where fluid and gas plays a major role in gaining a higher order of efficiencies. In fluid dynamics the computer simulations features a very accurate flow in and around the various objects which are very unmanageable, financially inefficient and very tough or almost impossible to measure or visualise experimentally by conventional methods. While, developing the simulation the transition phase from laminar to turbulent plays a vital role in determination of Drag and Lift component of the Airfoil. Thus, modelling a proper turbulence model will definitely produce an accurate value of drag.

The focal point in computational fluid dynamics is to numerically solve the Navier-Stokes equations which includes the transport of mass, momentum and energy in the flow field. The standard k epsilon (k-ε) and k-omega (k-ω)is employed to determine the separation of boundary layer on TsAGI -12% Airfoil.

The initial level in modelling a problem, demands the development of the geometry of the interested body, in case of Airfoil one may import the coordinate data file of the required Airfoil, after the development of the Airfoil geometry, a domain boundary or enclosure is develop. The geometry completion further reaches a very vital stage called meshing. In meshing, the whole geometry is distributed into structured and unstructured cells, both geometry and meshing is developed with the pre-processor. The majority of the time is consecrated toward the mesh generation for the domain geometry. Mesh generation is the deciding factor between the desired accuracy and solution cost. The mesh generation is also sized and refined for a higher degree of accuracy, by increasing in the number of structured cells. After the creation of the grid rest of the mathematics works is rendered to the solver, solver is able to solve the governing equations of different turbulence models. The procedurefor solving the problem are as follows: first the modelling has to be defined and the geometry and mesh is generated in

per-processor, furthermore the regions has to be specified in the geometry. Then physical models are defined in the models with desired circumstances like Ncrit, Reynolds number etc. after setting up all the boundary conditions the iterations is defined, iterations is being iterated till a constant (negligibly varying) value is achieved. The last stage is converting the mathematical expressed values, into Graphs and Plots, coloured contour, streamlines, forces vectors graph were one can easily save the required values or graphs. Figure 1 provides a better illustration of the per-processing and post-processing in the Ansys 15.0. In this study the curves of lift and drag of the Airfoil is developed. The TsAGI-12% is chose because of the Airfoil has been used extensively in many Russian construction. Typical example of such use of Airfoil the Antonov, T-101, MiG-21.

II. INTRODUCTION TO TURBULENCE MODELS

"Turbulence is an irregular motion which in general makes its appearance in fluids, gaseous or liquid when they flow past solid surfaces or even when neighbouring streams of the same fluid flow past or over one another". This the definition of turbulence modelling developed by Taylor and Von Karman in1937 [1].

Research on turbulence modelling has much over increased in importance over the past years and has been considered to be the key concept in the computational determination of high Reynolds number flow in Computational fluid dynamics solvers. It is important to study the performance of different turbulence model for prediction of the laminar-turbulent transitional flow in the boundary layer of streamlined bodies of interest in the aerospace domain or fluid dynamics. Turbulence models are considered within the range of varying equation as follows:

- One-equation model as, Spalart-Allmaras
- Two-equation mode as, k-epsilon and k-omega.
- Three-equation model as, kkl-omega.
- Four-equation model as, transition SST.
- Seven-equation model as, Reynolds shear stress.
- LES (large eddies solver) & DES.

This model produces repellent results in the determination of the friction and pressure drag components as well as prediction of lift in the transition from laminar to turbulent flows. Before moving forward to the numerical analysis of tubule modelling, it is significant to investigate the history of it. The following history is provided by Ismail Celik [1]:

"The origin of the time-averaged Navier-Stokes equations dates back to the late nineteenth century when Reynolds (1895) published results from his research on turbulence. The earliest attempts at developing a mathematical description of turbulent stresses, which is the core of the closure problem, were performed by Boussinesq (1877) with the introduction of the eddy viscosity concept. Neither of these authors, however, attempted to solve the time-averaged Navier-Stokes equations in any kind of systematic manner. More information regarding the physics of viscous flow was still required, until Prandtl's discovery of the boundary layer in 1904. Prandtl (1925) later introduced the concept of mixing-length model, which prescribed an algebraic relation for the turbulent stresses. This early development was the cornerstone for nearby all turbulence modelling efforts for the next twenty years. The mixing length model is now known as an algebraic, or zero-equation model. To develop a more realistic mathematical model of the turbulent stresses, Prandtl (1945) introduced the first one-equation model by proposing that the eddy viscosity depends on the turbulent kinetic energy, k, solving a differential equation to approximate the exact equation for k. this one-equation model improved the turbulence prediction by taking into account the effect of flow history. The problem of specifying a turbulence length scale still remained. This info ,which can be thought of as a characteristics scale of the turbulent eddies, changes for different flows, and thus is required for a much complete description of turbulence. A much complete model would be one that can be applied to a given turbulent flow by prescribing boundary and/ or initial conditions.

Kolmogorov (1942) introduce the first complete turbulence model, by modelling the turbulent kinetic energy k, and introduced a second parameter ωthat he referred to as the rate of dissipation of energy per unit volume and time. This two-equation model, termed the k-ω model, used the reciprocal of ω 1 2 k served as a turbulence length scale, solving a differential equation for *omega* similar to the solution method for k. because of the complexity of the mathematics, which required the solution of non-linear differential equations, it went virtually without application for many years, before the availability of computers. Rotta (1951) pioneered the use of the Boussinesq approximation in turbulence models to solve for the Reynolds stresses. This approach is called a second-order or second-moment closure. Such model naturally incorporates non-local and history effects, such as streamline curvature and body forces . The previous eddy viscosity models failed to account for such effects. For a three-dimensional flow, these second-order closure models introduce seven equations, one for a turbulence length scale, and six for the Reynolds stresses. As with Kolmogorov's k-ω model, the complex nature of this model awaited adequate computer resources.

Thus by early 1950's, four main categories of turbulence models had developed:

1) Algebraic (Zero-Equation) models
2) One-Equation models
3) Two-Equation models
4) Second Equation models

With increased computer capabilities beginning in the 1960's, further development of all four of these classes of turbulence models has occurred [1]."

III. OVERVIEW OF THE TURBULENCE MODELS

A. *The k-epsilon model*

The k-epsilon model was first proposed by Harlow and Nakayama in 1968 [6] where k is the kinetic energy and epsilon is dissipation rate of turbulent kinetic energy k. this model is used for the system that affect the turbulent kinetic energy [2]. the governing equations of the model can be obtained from averaged Navier-Stokes equation for incompressible flows which describe before and it is as follows[5]:

$$\rho\frac{\partial\bar{u_i}}{\partial t}+\Sigma_j\left(\rho\bar{u_j}\frac{\partial\bar{u_j}}{\partial x_j}+\rho\frac{\bar{\partial}\bar{u'}_i}{x_j}u'_j\right)=\frac{-\partial\bar{p}}{-\partial x_i}+\Sigma_j\frac{\partial\bar{\tau_{ij}}}{\partial x_j}\ (1.1)$$

Where u is the velocity field and p is the pressure field. If the Navier-Stokes equation is multiplied by u_i and then the resulting equation is averaged the following formula can be derived:

$$\rho\frac{\bar{\partial}\bar{u_i}}{\partial t}u_i+\Sigma_j u_j\frac{\bar{\partial}\bar{\rho}\bar{u_i}}{\partial x_j}u_i=\frac{-\bar{\partial}\bar{p}}{\partial x_i}u_i+\Sigma_j\frac{\bar{\partial}\bar{\tau_{ij}}}{\partial x_j}u_i \quad (1.2)$$

When averaged Navier-Stokes equation was multiplied by $\bar{u}_i$ the resultant is:

$$\rho\frac{\partial\bar{u_i}}{\partial t}\bar{u_i}+\Sigma_j\left(\rho\bar{u_j}\frac{\partial\bar{u_i}}{\partial x_j}\bar{u_i}+\rho\frac{\bar{\partial}\bar{u'}_i}{x_j}u'_j\bar{u_i}\right)=-\partial\bar{u_i}+\Sigma_j\frac{\partial\bar{\tau_{ij}}}{\partial x_j}\bar{u_i} \quad (1.3)$$

$\tau_{ij}=-\rho\bar{u_i}\bar{u_j}$, so the formula take the form of:

$$\rho\frac{\partial\bar{u_i}}{\partial t}+\rho\Sigma_j\left(\bar{u_j}\frac{\partial\bar{u_i}}{\partial x_j}\bar{u_i}\right)=\frac{-\partial\bar{p}}{-\partial x_i}\bar{u_i}+\Sigma_j\frac{\partial\bar{\tau_{ij}}}{\partial x_j}\bar{u_i}+\frac{\partial\tau_{ij}}{\partial x_j}\bar{u_i} \quad (1.4)$$

When the equation (1.4) is subtracted from equation (1.3), the result given by:

$$\rho\frac{\bar{\partial}\bar{u'_i}}{\partial t}u'_i+\rho\Sigma_j\left(\bar{u_j}\frac{\partial\bar{u_i}}{\partial x_j}\bar{u_i}-\bar{u_j}\frac{\partial\bar{u_i}}{\partial x_j}\bar{u_i}\right)=\frac{-\partial\bar{p}}{-\partial x_i}\bar{u'_i}+\Sigma_j\left(\frac{\partial\bar{\tau_{ij}}}{\partial x_j}u'_i-\frac{\partial\tau_{ij}}{\partial x_j}\bar{u_i}\right) \quad (1.5)$$

When the averaging rules are applied, the after modified can be written as:

$$\frac{\rho}{2}\left(\frac{\bar{\partial}(\bar{u'}_i)^2}{\partial t}+\Sigma_j\frac{(\partial\bar{u'}_i)^2}{\partial x_j}-u'_j\right)=\frac{-\partial\bar{p'}}{-\partial x_i}\bar{u'}_i+\frac{\rho}{2}\Sigma_j\partial\frac{\left(\bar{u'}_i^2\bar{u'}_j^2\right)}{\partial x_j} \quad (1.6)$$

The instantaneous kinetic energy k(t) of a turbulent flow is the sum of the mean kinetic energy, $K=\frac{1}{2}(u^2+v^2+w^2)$ and the turbulent kinetic energy is, $K=\frac{1}{2}\left(\bar{u'^2}+\bar{v'^2}+\bar{w^2}\right)$ .The governing equation for k can be represented as follows [2]:

$$\partial\frac{(\rho k)}{\partial t}+div(\rho kU)=div\left(-\bar{p'}\bar{u'}+2\mu\bar{u'}\bar{s'}_{ij}-\rho\frac{1}{2}\bar{u'}_i\bar{u'}_i\bar{u'}_j\right)-2\mu\bar{s'}_{ij}\bar{s'}_{ij}+\rho\bar{u_i}\bar{u_j}\bar{s'}_{ij} \quad (1.7)$$

The viscous stress effects on k have two parts: is the $2\mu Us_{ij}$ transport of k because of the viscous stresses and is the viscous dissipation of the kinetic energy, k. The term $\rho U\bar{u'}_i\bar{u'}_j$ and $\rho\bar{u'}_i\bar{u'}_j.s_{ij}$ consists of Reynolds stresses and the first one the transport of k dues to the Reynolds stresses and the second one is the total decrease of k which occurs because of deformation. In high Reynolds numbers, the transport of k and the total decrease of k are quite larger than the viscous parts of the equation [2].

Advantages:

- Simplest turbulence model for which only initial or boundary conditions are needed to be supplied.
- Excellent performance for many industrially relevant flows.
- Well established, most widely validated turbulence model.

Disadvantages:

- More expensive to implement than mixing length model.

- Poor performance in some unconfined flows, flows with large extra strains (e.g. swirling flows), rotating flows, flows driven by anisotropy of normal Reynolds stresses.

B. Menter SST k omega model

k-omega SST model is a model to be used in the sub-layer of the boundary layer. The difference of this model from the other models is that it does not include damping functions and it is superior Wilcox ***k-ω*** model since it is more accurate. The ***k-ε*** model is the independent from the free stream values in the outer region of the boundary layer and Menter [3] used the ***k-ε*** formulation to propose the new model. The governing equation for k-omega SST model is as follows [2]:

$$\partial\frac{(\rho\omega)}{\partial t} + div(\rho\omega U) = div\left[\mu + \frac{\mu_t}{\sigma_{\omega,1}} grad(\omega)\right] + \gamma_2\left(2\rho S_{ij}.S_{ij} - \frac{2}{3}\rho\omega\frac{\partial U_i}{\partial x_j}\delta_{ij}\right) - \beta_2\rho\omega^2 + 2\frac{\rho}{\sigma_{\omega,2\omega}}\frac{\partial k}{\partial x_k}.\frac{\partial\omega}{\partial x_k} \quad (2.16)$$

The k-omega model also has two equations and eddy viscosity which have to be defined for CFD analysis. The formulas are as follows [3]:

$$k = \frac{2}{3}\left(U_{ref}\, I\right)^2 \quad (2.17)$$

$$\omega = C_\mu - \frac{\frac{1}{4}\sqrt{k}}{l} \quad (2.18)$$

$$V_t = \frac{k}{\omega} \quad (2.19)$$

Model constants are same as the ones provided in ***k-ε*** model. These equations are used for free stream. Considering the wall conditions, the following formulas are proposed [3]:

$$k_{wall} = 0 \quad (2.20)$$

$$\omega_{wall} = 10\frac{6\nu}{\beta(\Delta y)^2} \quad (2.21)$$

Where, β1= 0.075 and Δy is the distance of the centre of first cell.

C. Spalart-Allmaras

The Spalart-Allmaras model is one of the one-equation models and it includes only one transport equation for kinematic eddy viscosity parameter ν. The Spalart-Allmaras model provides promising results for external aerodynamics [2]. There has been made modifications on Spalart-Allmaras model but the baseline model will be discussed in this research. The transport equation and Reynolds stresses are as follows [7]:

$$\frac{D\tilde{\nu}}{Dt} = P - D = T + \frac{1}{\sigma}\left[\nabla.\left((\nu + \tilde{\nu})\right)\Delta\tilde{\nu} + C_{b2}(\nabla\eta\tilde{\nu})\right]^2 \quad (2.22)$$

Where, P is the production term, D is the wall destruction term and T is the trip term and they are given by:

$$P = C_{b1}(1 - f_{t2})\tilde{S}\tilde{\nu} \quad (2.23)$$

$$D = \left(C_{w1}f_w - \frac{C_{b1}}{k^2d^2}f_{t2}\right)\left[\frac{\tilde{\nu}}{d}\right]^2 \quad (2.24)$$

$$T = f_{t1}(\Delta u)^2 \quad (2.25)$$

Where S is the modified vortices and given by:

$$S = S + \frac{\tilde{\nu}}{k^2d^2}f_{v2} \quad (2.26)$$

IV. COMPUTATIONAL METHOD

In this report,TsAGI "B" series-12% Airfoil is utilised. TsAGI operates under Ministry Of Aviation (MAP), Russia. TsAGI is situated in Moscow, Russia and responsible for the designing, research, and development of the bureau like Mikoyan, it also conducts the flight test of Aircraft. TsAGI had it's foundation in 1918 and is currently known as Central Aerohydrodynamic Institute (CAI) which is named after Prof. N.E. Zhukovsky. The TsAGI "B" series-12% Airfoil is symmetric; the "B" series indicates that it has 2.012% (f/c). The -12% indicates that the Airfoil has 12% thickness to chord length ratio; it is 12% as thick as it is long. Reynolds number for the simulations is Re=1*10^6 same with reliable experimental data provide on the TsAGI website and MH Aero Tool, Javafoil. The free stream temperature is 288.16 K, approximately same as the temperature experienced by the aircraft when flying in the upper atmosphere. The density of the air at the mentioned temperature is, ρ=1.225 kg/m^3, and the viscosity is μ=1.7894E-05. The flow is considered incompressible at the described Reynolds number also; the ratio of specific heats is 1.4. The solver utilised is Implicit with AUSM flux type also the least square cell based gradient is employed. Courant Number of 5 is employed under-relaxation factors of 0.8 Turbulent Kinetic Energy. Calculations are made on the various angle of attack (AOA), ranging from 0 degrees to 19 degrees. The Airfoil profiles and coordinates are

imported from MH Aero Tool, Javafoil. There is 51 coordinate point are used to create the Airfoil profile. The mesh is created in per-processor of Ansys 15.0 which produces various structured and unstructured cells and nodes for the geometry of interest. The Airfoil is enclosed within a domain boundary. Cartesian coordinate system is employed in which centre of the Airfoil is pitched at the origin (0,0) of the coordinate system. The thickness of Airfoil is taken as, Y+ thus, the chord length is 8.3Y+. The domain is composed of a C-type grid of diameter of 121Y+ approaching to the leading edge of the Airfoil followed, by the rectangular grid of length 83Y+ and height of ±62.5Y+. The very first step in any CFD simulation is to check the effect of mesh size on the solution result. It is well known that very accurate results could be achieved by increasing the number of nodes in the grid. The appropriate number of nodes can be defined by the grid independence test; grid independence test refers to the refinement of the grid till a constant solution result is obtained. The non-dimensional grid spacing varies as Δ= 0.01-0.03741m. These values of spacing are satisfactorily good to capture the boundary layer separation. The computation was performed on a machine embedded with AMD A6 (quad-core) processor at a processing speed of 2.00 GHz. The schematic diagram is provided below for better understanding of the problem

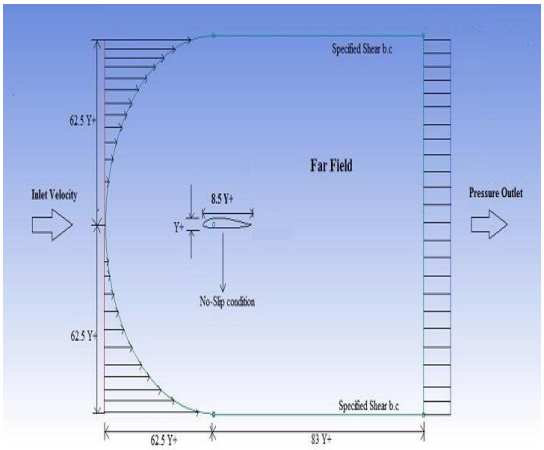

Fig 1: Schematic diagram of flow geometry with boundary conditions

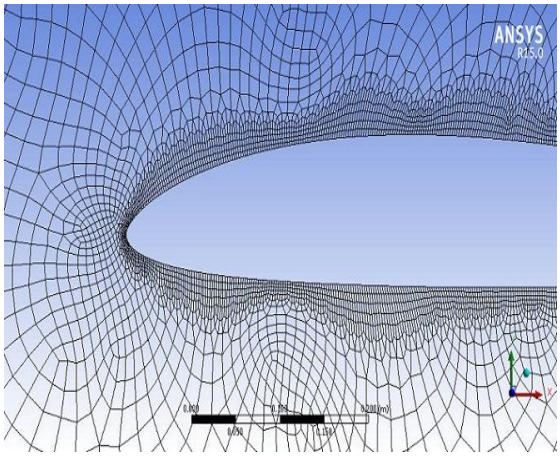

Fig 2: Refined mesh near Airfoil

V. RESULTS AND DISCUSSION

To visualise the results and compare it with earlier experimentally performed data from reliable resources, the simulations for the different angle of attack on various turbulence models is performed. The simulations are made with a range of various angle of attack from 0 º to 19 º.

In Fluid mechanics whenever there is a relative velocity between a solid body and viscous fluid surrounding it, the body will experience a net force F. the magnitude of this force depends upon many factors such as, velocity of fluid, properties of fluid (e.g. Density, viscosity, etc.) and also on the shape and sizes of the immersed body. Due to the flow of the Fluid around the body, it establishes stresses on each element of the body surface and leads to some net force. The stresses are composed of tangential stresses due to the viscous action of fluid and normal stresses developed due to local pressure. It is found that by integrating the viscous stresses over the body surface we can obtain the contribution to the net force F. Therefore, then net force F_{NET} can be decomposed into drag force, F_D ; as the force parallel to the motion of the fluid and into lift force, F_L; the force normal to the surface of the body. For a better and sensible illustration of the results the calculated value are converted into a graph. Figure 3 is the graph of coefficient of lift against the angle of attack, computed with four turbulence model and compared with the reference data. The graph is evident that there is a linear relation between the lift coefficient and the angle of attack but this situation could be only be maintained at a low angle of attack.

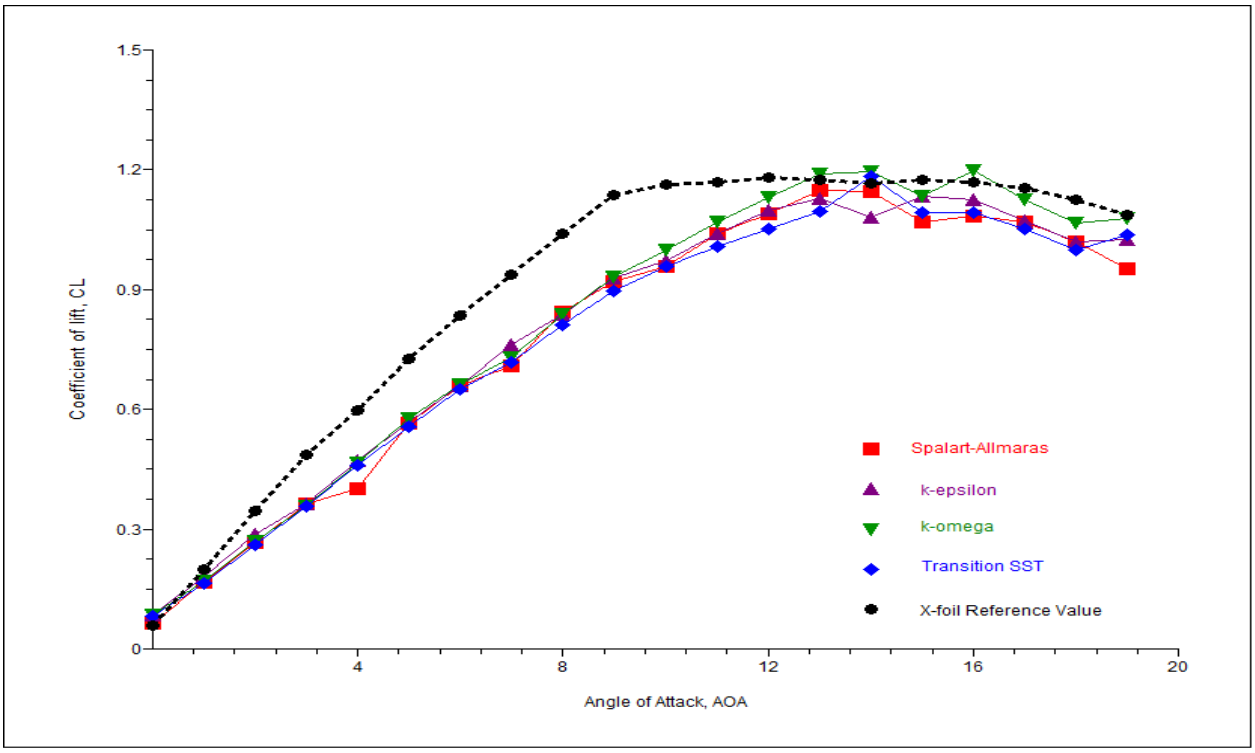

Fig 3: Comparison between the reference data from x-foil and the four different turbulence models simulation results of the lift coefficient curve

Further, increase in angle of attack, the pressure difference between the upper and lower surfaces increases, causing the lift coefficient to increase smoothly until a maximum is reached further increase in angle of attack results in sudden drop of lift coefficient also, the flow separation on major surface is visible, in fluid mechanics this situation is called *Stall.*

The stall condition is visible at 15°. As the stall increased the disagreement between the data is seen. The lift coefficient drops and the drag increase gradually as shown in figure 4.

The values of drag coefficient of all four turbulence model is very close to the experimented data. The most accurate model from the study is k-ω Standard, second came the k-ε standard, third, stands the Spalart-Allmaras model and the least accurate is transition SST turbulence model.

Plots between lift coefficients against drag coefficient are also given in fig 5 graph between lift and drag is also called lift-drag polar. The ratio of C_L and $_D$ or lift/drag ratio is one of the key points while designing of an aircraft. The lift determines the amount of load that can be carried by aircraft and the drag determines the amount work done by aircraft engine in order to generate the needed lift.

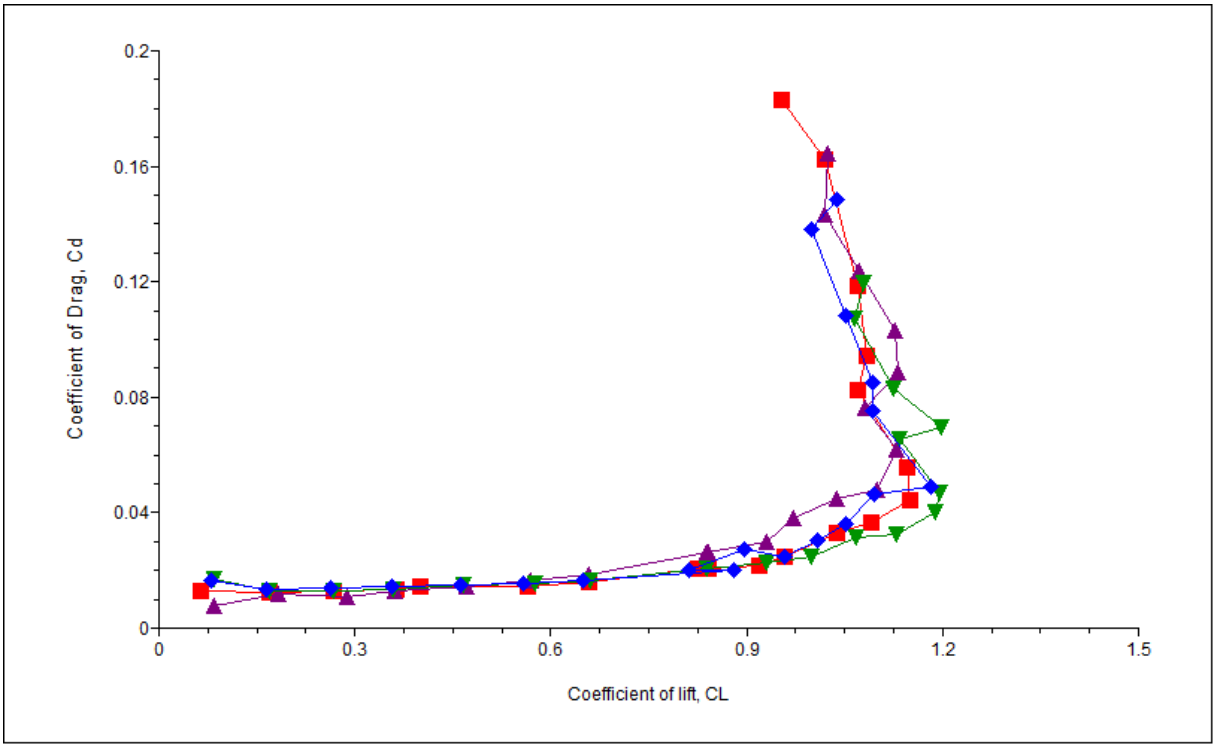

Fig 4: Comparison of Drag coefficient against various angles of attack

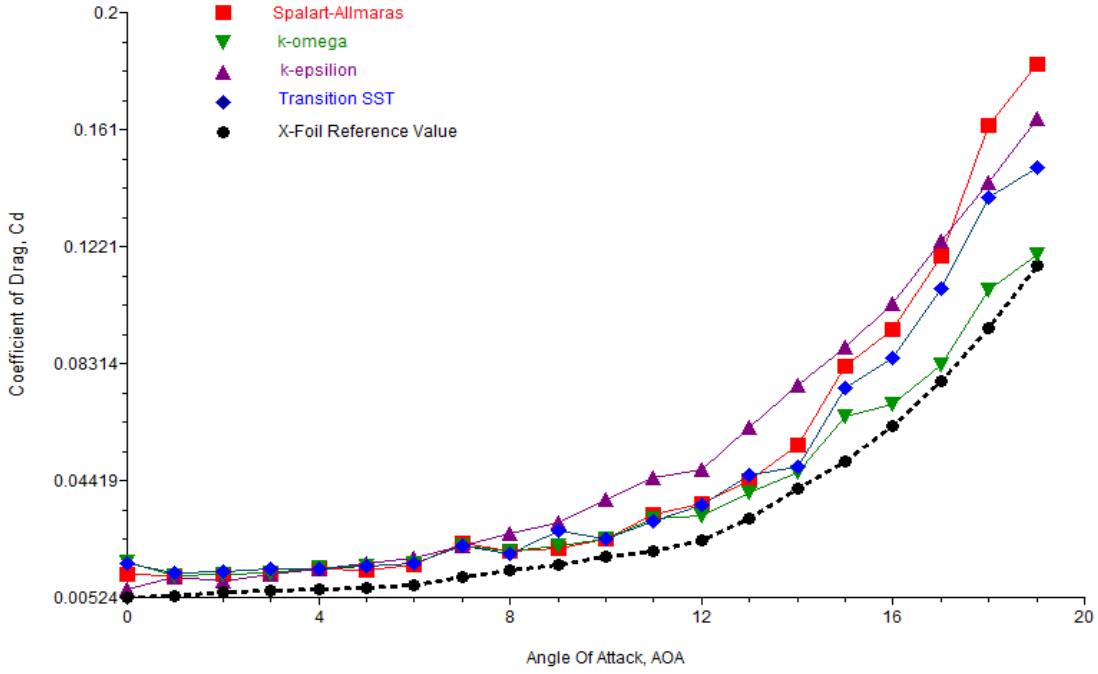

Fig 5: Lift-Drag polar

From the lift drag-polar it is clear that the calculated drag is higher that the experimental data. The higher value of drag is expected earlier since the actual Airfoil does not goes through a fully turbulent flow but laminar at the forward half.

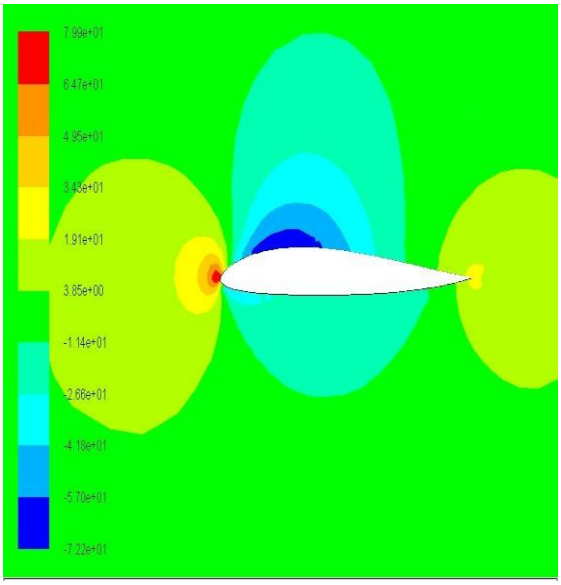

Fig 6: Static pressure contour at 0° AOA with k-omega turbulence model

At 0° angle of attack the static pressure contours the pressure distribution is symmetric on the upper as well as the lower surface of Airfoil therefore, it can be concluded that the flow is symmetric and the stagnation point is same for upper surface as well as for lower surface of Airfoil. Static pressure contours at 0° is shown in figure 6.

Figure 7, 8 and 9 shows the static pressure contours at 3°, 6° and 9° with k-omega turbulence model. From the figure 7, 8 and 9 it is evident that the pressure distribution on the lower surface is higher than the pressure of the incoming flow furthermore, the upper surface has a low- pressure distribution compared to the incoming flow. Thus, it can be concluded that the higher pressure on the lower surface tends to push the Airfoil in the upper direction which combines with the literature of any fluid mechanics text would refer this phenomenon as the generation of lift, C_L.

The velocity contours at angle 3°, 6° and 9° are also shown in the figure. In the given contours (fig 10, 11 and 12) the leading edge stagnation point (stagnation point is the point in the flow field where the local velocity of fluid is zero) at low angle attack the stagnation point is near the leading edge and as the angle of attack increases the stagnation point starts approaching toward the trailing edge. Similarly, on the other hand the trailing edge stagnation point at the low angle of attack it establishes itself on the forward of the Airfoil and as the angle of attack increases, it starts shifting itself to the leading edge.

Figure 8, 9 and 10 shows the static pressure contours at 3°, 6° and 9° with k-omega turbulence model. From the figure 8, 9 and 10 it is evident that the pressure distribution on the lower surface is higher than the pressure of the incoming flow furthermore, the upper surface has a low- pressure distribution compared to the incoming flow. Thus, it can be concluded that the higher pressure on the lower surface tends to push the Airfoil in the upper direction which combines with the literature of any fluid mechanics text would refer this phenomenon as the generation of lift, C_L.

The velocity contours at angle 3°, 6° and 9° are also shown in the figure. In the given contours (fig 11, 12 and 13) the leading edge stagnation point (stagnation point is the point in the flow field where the local velocity of fluid is zero) at low angle attack the stagnation point is near the leading edge and as the angle of attack increases the stagnation point starts approaching toward the trailing edge. Similarly, on the other hand the trailing edge stagnation point at the low angle of attack it establishes itself on the forward of the airfoil and as the angle of attack increases, it starts shifting itself to the leading edge.

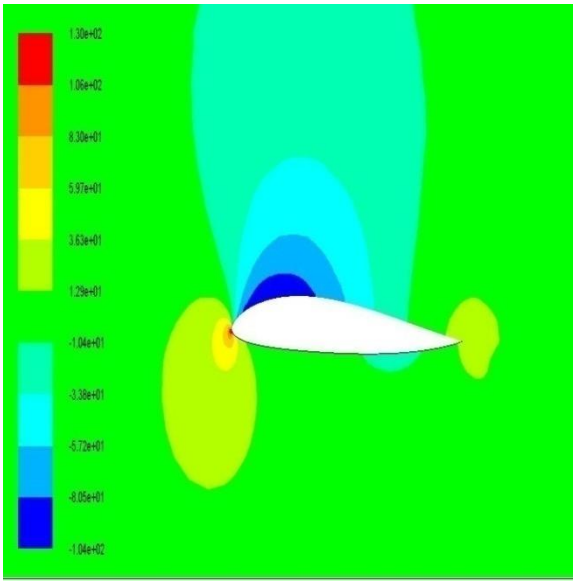

Fig 7: Static pressure contours at 3° AOA with k-omega turbulence model

Figure10,11 and 12 shows that velocity on the upper surface of the Airfoil is much greater than the lower surface which is desirable and needed to create a higher pressure regime on the lower surface and low pressure regime on the upper surface of the Airfoil.

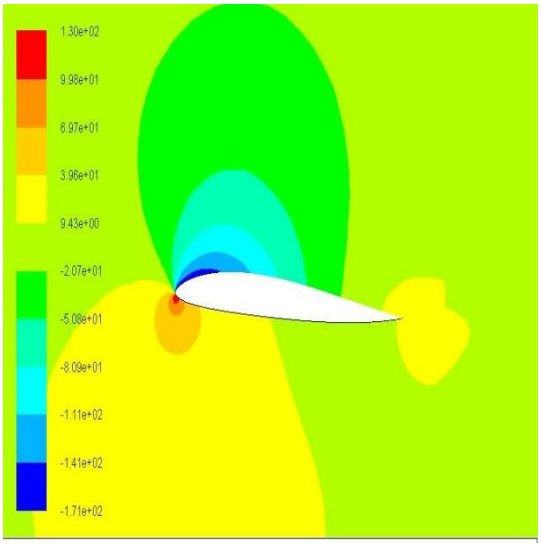

Fig 8: static pressure contours at 6° AOA with k-omega turbulence model.

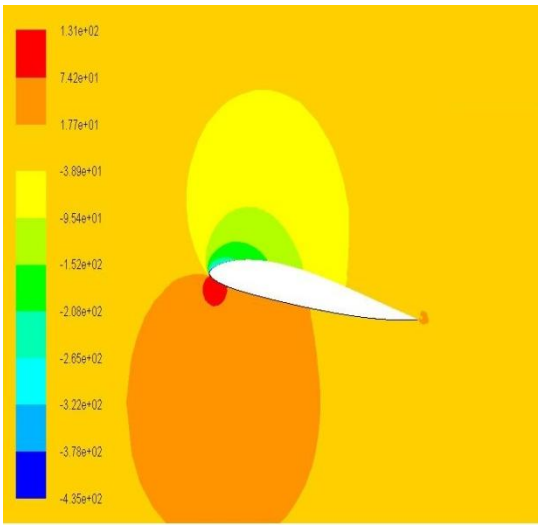

Fig 9: Static pressure contours at 9° AOA with k-omega turbulence model.

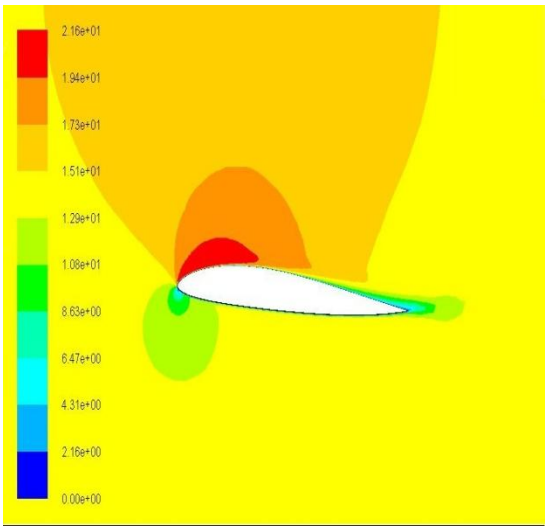

Fig 10: Velocity contour at 3° AOA with k-omega turbulence model.

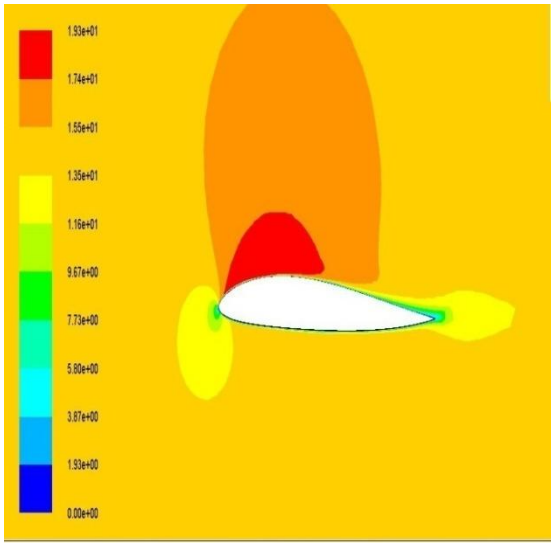

Fig 11: Velocity contour at 6° AOA with k-omega turbulence model

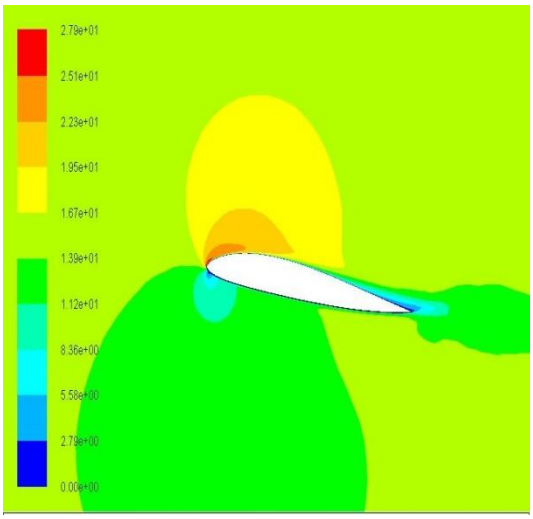

Fig 12: Velocity contour at 9° AOA with k-omega turbulence model

VI. CONCLUSION

In this paper, the simulation of TsAGI "B" series is shown with four different turbulence models thus, from the calculated results it can be concluded that the most appropriate turbulence model was *k-ω* standard, two equation model. It is also concluded that the drag coefficient is greater than the reference value. This was because the actual Airfoil experiences a laminar flow over the forward half.

REFERENCES

[1] Ismail B. Celik. Introductory turbulence modeling. Technical report, West Virginia University,Mechanical Engineering Department, 1999.

[2] H K Versteeg and Malalasekera W. An introduction to Computational Fluid Dynamic, The Finite Volume Method Second edition. Pearson Education Limited 1995, 2007.

[3] F. R. Menter. Two-equation eddy-viscosity turbulence models for engineering applications. Pages 330-331, 1994.
[4] J. N. Newman. Marine Hydrodynamics. The MIT Press, 1977.
[5] Colleen D. Scott-Pomerantz. The k-epsilon model in the theory of turbulence. Technical report, University of Pittsburgh, 2004.
[6] Nakayama P.I. Harlow, F. R. Transport of turbulence energy decay rate. 1968.
[7] Abbott IH, Von Doenhoff AE (1959). Theory of Wing Sections. Dover Publishing, New York.
[8] Bacha WA, Ghaly WS (2006). Drag Prediction in Transitional Flow over Two-Dimensional Airfoils, Proceedings of the 44th AIAA Aerospace Sciences Meeting and Exhibit, Reno, NV.
[9] S.L. Chernyshev, A.Ph. Kiselev n, A.P. Kuryachii , Laminar flow control research at TsAGI: Past and present , Page 170, 172, 175, 179.
[10] Badran O (2008). Formulation of Two-Equation Turbulence Models for Turbulent Flow over a NACA 4412 Airfoil at Angle of Attack 15 Degree, 6th International Colloquium on Bluff Bodies Aerodynamics and Applications, Milano, 20-24 July.
[11] Michael S. Selig, James J. Guglielmo, Andy P. Broeren and Philippe Giguere ,Summary of Low-Speed Airfoil Data volume 1, Univrsity of Illinois, Soar Tech Publication, Virginia beach, Virginia.
[12] Scott Richards, Keith Martin, and John M. Cimbala,, ANSYS Workbench Tutorial – Flow Over an Airfoil , Penn State University.
[13] Michael S. Selig, Robert W. Deters, and Gregory A. Williamson, Wind Tunnel Testing Airfoils at Low Reynolds Numbers , 49th AIAA Aerospace Sciences Meeting , Pages 4-11,
[14] Spalart, PR, Allmaras SR (1992). A One-Equation Turbulence Model for Aerodynamic Flows. AIAA Paper, pp. 92-439.
[15] Sutherland W (1893). The viscosity of gases and molecular force. Philosophical Magazine, S., 5, 36: 507-531.
[16] Mikhailov VV. Laminar–turbulent transition and boundary layer control. TsAGI—principal stages of scientific activities 1968–1993. Moscow: Nauka- Fizmatlit; 1996. p. 367 À 71 .
[17] Kuzminsky VA. Matrix numerical method of stability calculation of three- dimensional boundary layer. Uchenye Zapiski TsAGI 2007;38(3–4): 44–56.
[18] Kiselev APh, Bokser VD. Investigation of flow laminarization of swept wings. TsAGI—principal stages of scientific activities 1993—2003. Moscow: Nauka- Fizmatlit; 2003. p. 133 À 8
[19] Mig-23/27 Flogger in action, Squadron publication 1990.
[20] Shames, I. H., “Mechanics of Fluid”, 3rd Ed., Ch. 13: pp. 669-675.